Sheared salt fingers: Instability in a truncated system

Francesco Paparella and Edward A. Spiegel
Astronomy Department, Columbia University, New York, New York 10027

(Received 1 July 1998; accepted 20 January 1999)

We derive a model for fingering doubly diffusive convection from a truncated expansion in horizontal planform functions with the inclusion of a large-scale shearing mode. This produces nonlinear partial differential equations in time and in vertical coordinate. At a high enough Rayleigh number, both convection and shear modes are sustained and their interaction produces rich cyclic dynamics with the fingering layer dividing into two distinct finger layers that engender steps in the mean salinity before being disrupted by the beginning of a new cycle. © *1999 American Institute of Physics.* [S1070-6631(99)01305-7]

I. INTRODUCTION

Doubly diffusive convection occurs when two distinct fluid properties such as temperature or solute concentration with different diffusivities affect the buoyancy of a fluid. The resulting dynamics are especially enriched when these properties are spatially distributed in such a way that one is stabilizing and the other destabilizing in the gravitational field. Even when the total density is larger below, we may have instability.[1] When the two buoyancy-making properties are temperature and salinity, this form of convection is also called thermohaline convection. Following a well-established custom we shall call the more slowly diffusing property *salt* and the other *temperature*. In a particular range of parameters, the process is relevant to the modeling of stellar interiors in an advanced state of evolution and in those special circumstances (not treated here; see Ref. 2) the term semiconvection is used.

In certain parameter ranges of doubly diffusive convection, the motions take the form of narrow cells called salt fingers. This configuration allows the fluid to take advantage of the diffusive effects crucial to the maintenance of the unstable motions. A significant manifestation of fingering convection is found in the oceans where favorable conditions occur. As described in the review of Schmitt,[3] one often observes there the appearance and the persistence of steplike structures in the vertical profiles of temperature and salinity. An understanding of the formation of these structures would be of value in predicting transport properties and in deciding whether they may also occur in less observable conditions, as in stellar interiors.

Laboratory experiments show that a layer of fingers can divide along its mid-plane to produce two distinct fingering layers joined by a well mixed region in which a salt-driven convection takes place in motions on a much larger horizontal scale. The layer division may occur repeatedly under suitable conditions with a corresponding development of steplike vertical profiles of temperature and salinity. The well-mixed regions alternate with thinner layers of high gradients of temperature and salinity, corresponding to the finger zones. While the laboratory profiles are very reminiscent of the oceanic staircases in form, we should be mindful of the mismatch between their sizes and those of the laboratory measurements.

Layer formation has been attributed to various instabilities. Stern[4] suggested a collective instability of fingers that has been well studied.[5–7] In its original formulation, this instability originates when an array of infinitely tall salt fingers is perturbed by an internal wave. Kunze[7] proposed that the relevant mechanism is the shear between ascending and descending fingers, but his instability criterion reduces to that of Stern. However, not all the experiments confirm the results of the idealized models.

Some authors found instability when the vertical fluxes were about one order of magnitude less than those required to trigger the collective instability.[8,9] Further analysis by Holyer[6] suggested that a set of infinitely tall salt fingers may undergo a ''nonoscillatory'' instability, arising rather from vertical shearing motions. These are a thermohaline analogue of the vertical shears detected in the large scale motions in ordinary convection by Krishnamurti and Howard.[10] The importance of such shearing motions is confirmed by the observation of strongly tilted convective fingers in the ocean such as one would expect to find in the presence of an intense vertical shear.[3]

The problem of salt fingers in an external shear was addressed by Linden.[11] For high Richardson numbers and low Rayleigh numbers, he showed from both finite-amplitude calculations and laboratory experiments that a roll planform is preferred. The rolls subsequently give rise to an array of salinity sheets aligned downshear. Kunze,[12] who included an externally driven shear in his previous model,[7] suggested that finger instability would occur when a *hybrid wave/finger Froude number* exceeds a critical value. However, he deduced a relation between shear strength and vertical flux in disagreement with Linden's experiments.

In ordinary convection, the shearing motions become significant only at relatively high Rayleigh numbers. In that context, it has been found revealing to study these large scale motions with simplified models derived from modal truncation, as was first done by Howard and Krishnamurti[13] and enlarged in later works.[14,15] Like the Lorenz model of thermal convection,[16] these are low order truncations of the Fou-

rier series for the fields in both the horizontal and the vertical directions. By contrast, since the features of interest here involve intricacies of the vertical structure, in the present work we truncate *only* the horizontal expansions and keep the full vertical structure in our description.

Horizontally truncated expansions have proved useful in several fluid problems including Poiseuille flow[17] and Rayleigh–Bénard convection.[18,19] They have also been used in doubly diffusive convection[20] but the large scale flows were not included in those studies. As we shall see, the shearing flows modify the finger dynamics significantly.

While truncated models have certain limitations, as the earlier studies have shown, they are very useful for exploratory purposes and can quickly reveal the kinds of phenomena one can expect. Once the interesting aspects have been isolated, they can be followed up with full simulations in the specific cases of greatest interest. Indeed, we shall later provide such results from direct simulation to buttress our present findings, but no direct simulations for conditions in the oceans and stellar interiors are likely to be possible very soon and the modal approach should continue to provide guidance in such problems.

In the next section we describe our modal approach to thermohaline convection. Then in Sec. III, we outline some of the numerical results obtained with the modal equations and the effects of shear on them. In particular, we describe the salt finger instability induced by shear. We end with a discussion in Sec. IV.

II. A SINGLE-MODE MODEL

The rationale of the modal approach pursued here is that the net transport and much of dynamics is controlled by the vertical profiles of temperature and salinity so that it is important to try to be accurate in their description. The deformation of these profiles by the motions provides one of the principal nonlinear effects controlling the dynamics and we must aim to treat these in a self-consistent way. To do this with a minimal representation, we sacrifice accuracy in the horizontal structures by drastically truncating in an expansion in horizontal normal modes. The resulting truncated system is a set of model equations of a kind that has often proved useful in exploratory discussions (see references in the previous section) while not requiring great computational resources.

Here we restrict our attention to the two-dimensional, Boussinesq equations for doubly diffusive convection using a stream function ψ, with horizontal velocity $\partial_z\psi=u$ and vertical velocity $\partial_x\psi=-w$. The equations then are

$$\begin{aligned}
&\partial_t\boldsymbol{\nabla}^2\psi-J(\psi,\boldsymbol{\nabla}^2\psi)=-\sigma R_T\partial_x T+\sigma R_S\partial_x S+\sigma\boldsymbol{\nabla}^4\psi,\\
&\partial_t T-J(\psi,T)=\boldsymbol{\nabla}^2 T,\\
&\partial_t S-J(\psi,S)=\tau\boldsymbol{\nabla}^2 S.
\end{aligned}\tag{1}$$

The fluid is confined between two infinite horizontal, rigid plates, separated by a distance πd. The equations have been made dimensionless using d as the scale of length, d^2/κ_T as the scale of time, and ΔT and ΔS, the imposed differences of temperature and salinity across the slab, as units of temperature and salinity differences. The thermal and salinity Rayleigh numbers are defined conventionally as

$$R_T=\frac{g\alpha\Delta T d^3}{\kappa_T\nu}\quad\text{and}\quad R_S=\frac{g\beta\Delta S d^3}{\kappa_T\nu},\tag{2}$$

where α and β are the thermal and saline expansion coefficients, g is the gravity acceleration, ν is the kinematic viscosity, and κ_T is the thermal diffusivity. The Prandtl number and the reciprocal of the Lewis number are

$$\sigma=\frac{\nu}{\kappa_T}\quad\text{and}\quad\tau=\frac{\kappa_S}{\kappa_T},\tag{3}$$

where κ_S is the diffusivity of salt.

The fields ψ, T, and S are each split into a horizontally averaged part (denoted by a bar) and a fluctuating part (denoted by a prime):

$$\begin{aligned}
&\psi=\overline{\psi}(z,t)+\psi'(x,z,t),\\
&T=\overline{T}(z,t)+T'(x,z,t),\\
&S=\overline{S}(z,t)+S'(x,z,t).
\end{aligned}\tag{4}$$

The fluctuating fields are expanded as

$$\begin{aligned}
&w'=\int_a f_a(x)W_a(z,t)da,\\
&T'=\int_a f_a(x)\Theta_a(z,t)da,\\
&S'=\int_a f_a(x)\Phi_a(z,t)da.
\end{aligned}\tag{5}$$

The horizontal planform functions $f_a(x)$, which depend on the wave number, a, are solutions of the Helmholtz equation,

$$\partial_{xx}f_a=-af_a.\tag{6}$$

In our horizontally unlimited geometry, these are simply sines and cosines.

The expansions for the horizontal velocity and for the stream function are then found using the continuity equation, $\boldsymbol{\nabla}\cdot\mathbf{u}=0$. In solving for the stream function, we find that it may have a part which depends only on z, which corresponds to a shearing horizontal motion. This shearing motion had been rather neglected prior to the discovery by Krishnamurti and Howard[10,21] that such a motion is an intrinsic and important property of convection at high Rayleigh number. Indeed, in two dimensions, the first onset of shear is at high Rayleigh numbers, while in three dimensions, modal calculations reveal that it can occur weakly at the onset of convection.[22] The interpretation of this motion as a spontaneous symmetry breaking is possible.[13,23]

On substituting (4) and (5) into the Boussinesq Eq. (1), multiplying by $f_a(x)$, and averaging over x, one obtains an infinite set of coupled PDEs for the amplitudes W_a, Θ_a, Φ_a. These equations are equivalent to the starting Boussinesq equations, in the two dimensional case. Here we drastically simplify the modal equations by retaining only a single wave number, α, and so obtain the following set of nine PDEs in vertical coordinate and time:

$$
\begin{aligned}
\partial_t U &= \partial_z(\sigma\partial_z U + (1/\alpha)W^+\partial_z W^- - (1/\alpha)W^-\partial_z W^+),\\
\partial_t \overline{T} &= \partial_z(\partial_z \overline{T} - W^+\Theta^+ - W^-\Theta^-),\\
\partial_t \overline{S} &= \partial_z(\tau\partial_z \overline{S} - W^+\Phi^+ - W^-\Phi^-),\\
\partial_t \Theta^+ &= \mathcal{D}\Theta^+ + \alpha U\Theta^- - W^+\partial_z \overline{T},\\
\partial_t \Theta^- &= \mathcal{D}\Theta^- - \alpha U\Theta^+ - W^-\partial_z \overline{T},\\
\partial_t \Phi^+ &= \tau\mathcal{D}\Phi^+ + \alpha U\Phi^- - W^+\partial_z \overline{S},\\
\partial_t \Phi^- &= \tau\mathcal{D}\Phi^- - \alpha U\Phi^- - W^-\partial_z \overline{S},\\
\partial_t \mathcal{D}W^+ &= \sigma\mathcal{D}^2 W^+ - \sigma\alpha^2(R_T\Theta^+ - R_S\Phi^+)\\
&\quad - \alpha W^-\partial_{zz}U + \alpha U\mathcal{D}W^-,\\
\partial_t \mathcal{D}W^- &= \sigma\mathcal{D}^2 W^- - \sigma\alpha^2(R_T\Theta^- - R_S\Phi^-)\\
&\quad + \alpha W^+\partial_{zz}U - \alpha U\mathcal{D}W^+.
\end{aligned}
\tag{7}
$$

We have introduced the operator $\mathcal{D}=\partial_{zz}-\alpha^2$ and have set $U=\partial_z\psi$ where U represents a large-scale, shearing velocity. The variables with the superscript $^+$ are the amplitudes of $\cos(\alpha x)$, while the amplitudes of $\sin(\alpha x)$ have the $^-$ as superscript. The two kinds of amplitudes are coupled only through the equations for the averaged variables, T, S, and U.

III. NUMERICAL RESULTS

To solve the single-mode equations, we have used a pseudospectral code. This advances the diagonal, linear terms of the Eq. (7) in time in the Fourier space with the integrating factor technique, and the nonlinear or nondiagonal terms with a second-order Adams–Bashforth scheme.[24] To simplify the boundary conditions we split the averaged profiles of temperature and salinity as $\overline{T}=\tilde{T}+z$, and $\overline{S}=\tilde{S}+z$. The zero values on the top and bottom required by the boundary conditions have been imposed using a discrete sine transform for all the variables, except for U, which has a zero first derivative at the boundaries. The latter condition may be imposed by employing a discrete cosine transform.

A. The shear-induced finger instability

We have explored the numerical solution of the nine modal equation (7) in a large range of parameter values. We typically took initial conditions with horizontally averaged temperature and salinity profiles that mimic the initial two-layer setup used in many experiments, namely

$$
\overline{T}(z,0)=\overline{S}(z,0)=\frac{\pi}{1+\exp[\mu(\pi/2-z)]}. \tag{8}
$$

This form has no discontinuity between the upper and lower layer, but the transition is quite sharp since we use $\mu=10$. The amplitudes of the vertical velocity fluctuations were initially $W^+(z,0)=W^-(z,0)=A\sin(z)$, with $A=0.01$. Often the large scale flow was also initially excited as $U(z,0)=A\cos(z)$. The other variables were initially zero.

In Fig. 1 we show the results obtained with these initial conditions at time $t=0.5$. The parameter values used in this computation are $R_T=1000$, $R_S=667$, $\sigma=10$, and $\tau=0.1$ The wave number is $\alpha=4$, which is close to the fastest growing wave number of the linear theory. The quantities plotted are the stream function, the temperature, and the salinity fields, computed by putting the solutions of the nine modal equations into the expansions (5) and (4). The evolution of small initial perturbations generates tall, fingerlike plumes, alternatively ascending and descending. These grow until they reach the rigid upper or lower boundary, eventually forming a strong boundary layer in the salinity field, and a much weaker one in the temperature field as shown in Fig. 2. Slender convection cells are evident in the stream function field. The salinity field is mainly advected. Note the droplets of excess (deficient) salinity in the descending (ascending) plumes, reminiscent of what is believed to happen in the bulbous tips of actual salt fingers.[25] The temperature field is dominated by diffusion and can be described as a wave perturbation over the basic gradient state. The horizontally averaged profiles of temperature and salinity are shown in Fig. 3.

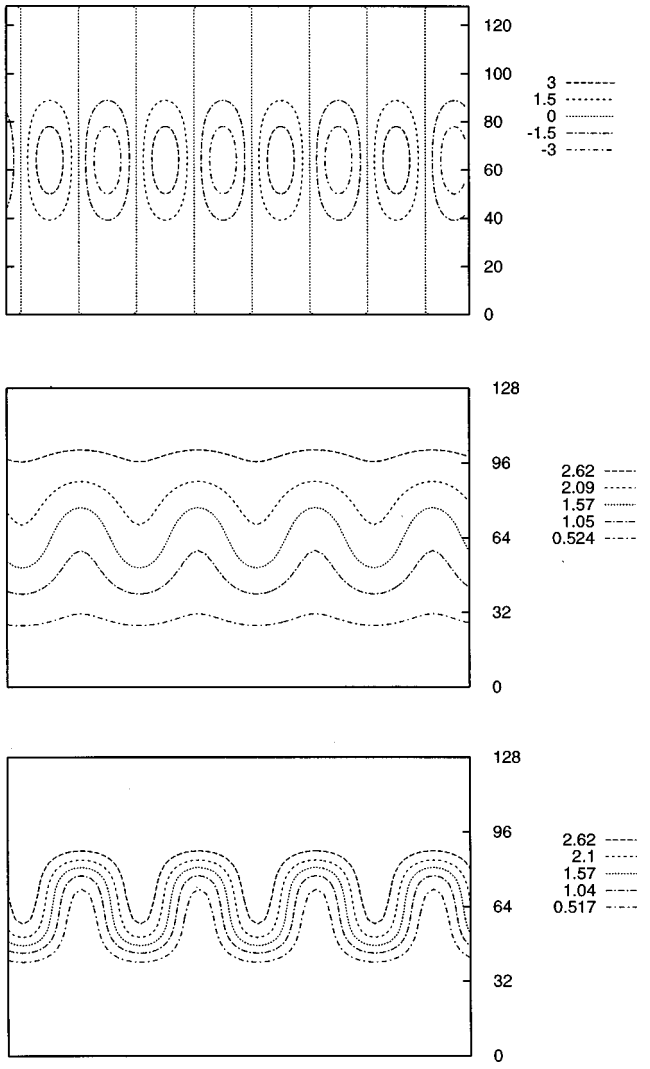

FIG. 1. Stream function, temperature, and salinity field (from top to bottom) at the time $t=0.5$. The domain height is π, its width is 2π. The units on the y axis are gridpoints. For the parameters of this simulation see the text.

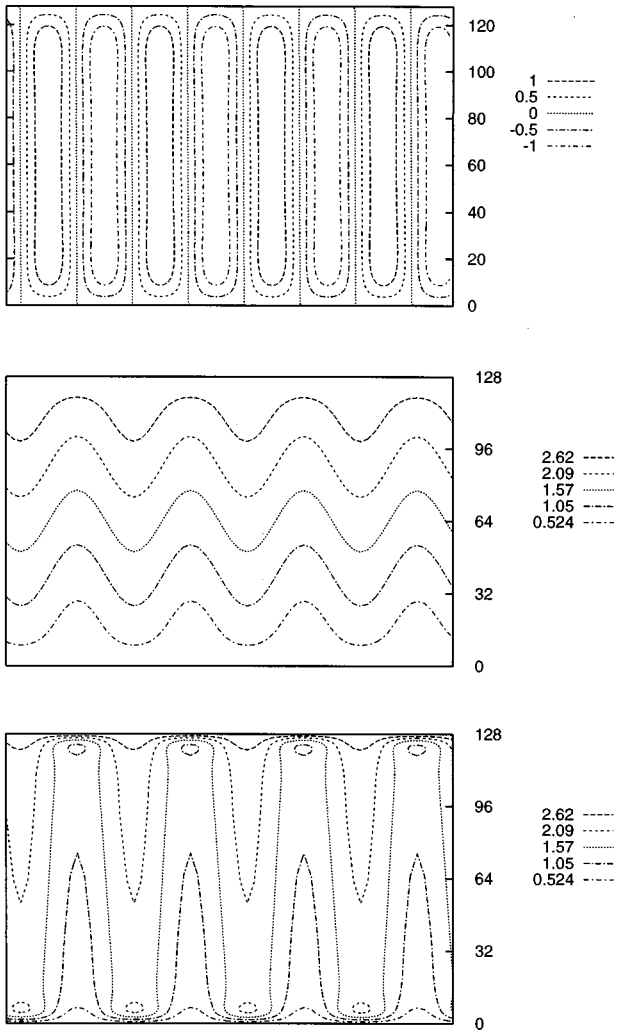

FIG. 2. Stream function, temperature, and salinity field (from top to bottom) at the time $t=5$. Same simulation as Fig. 1.

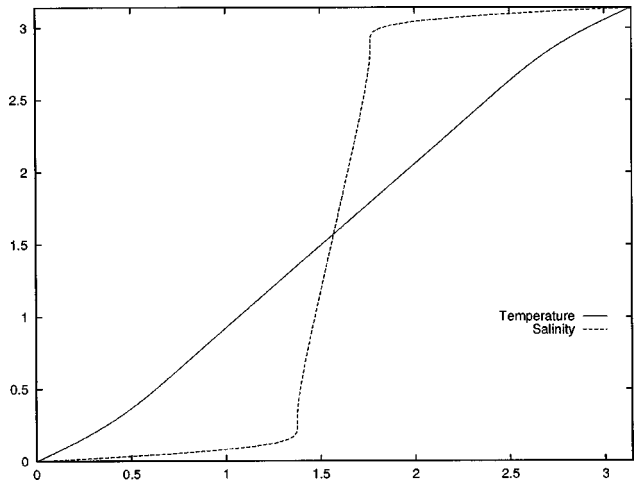

FIG. 3. Horizontally averaged temperature and salinity profiles of the fields shown in Fig. 2. The horizontal axis is dimensionless temperature and salinity. The vertical one is dimensionless height.

TABLE I. Asymptotic behavior of the solutions for $R_T=1000$, $\sigma=10$, $\tau=0.1$, and $\alpha=4$.

$\mathcal{R}_\rho$	1.5	2	3
	layering inst.	tilted cells	tilted cells
$\mathcal{R}_\rho$	4	5	6
	straight cells	straight cells	straight cells

Once this transient initial stage is completed, different evolutions are possible depending on the value of the density ratio

$$\mathcal{R}_\rho = R_T / R_S , \tag{9}$$

as summarized in Table I. At the highest density ratios, corresponding to a very stabilizing temperature difference, the convection cells remain steady and straight and no large-scale flow is generated. At smaller density ratios a large scale flow slowly grows and tilts the convection cells as in Fig. 4. For even smaller density ratios (but still greater than one) the large scale flow becomes periodic in time. In this regime, the temperature and salinity fields become horizontally homoge-

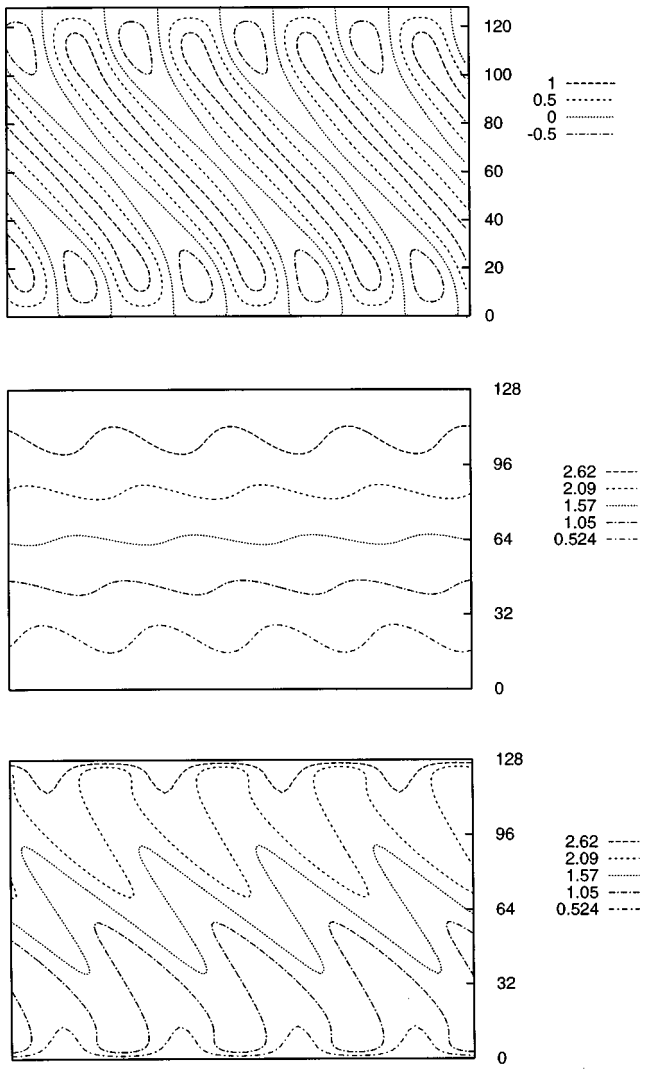

FIG. 4. Stream function, temperature, and salinity field (from top to bottom) at the time $t=10$. Same simulation as Fig. 1.

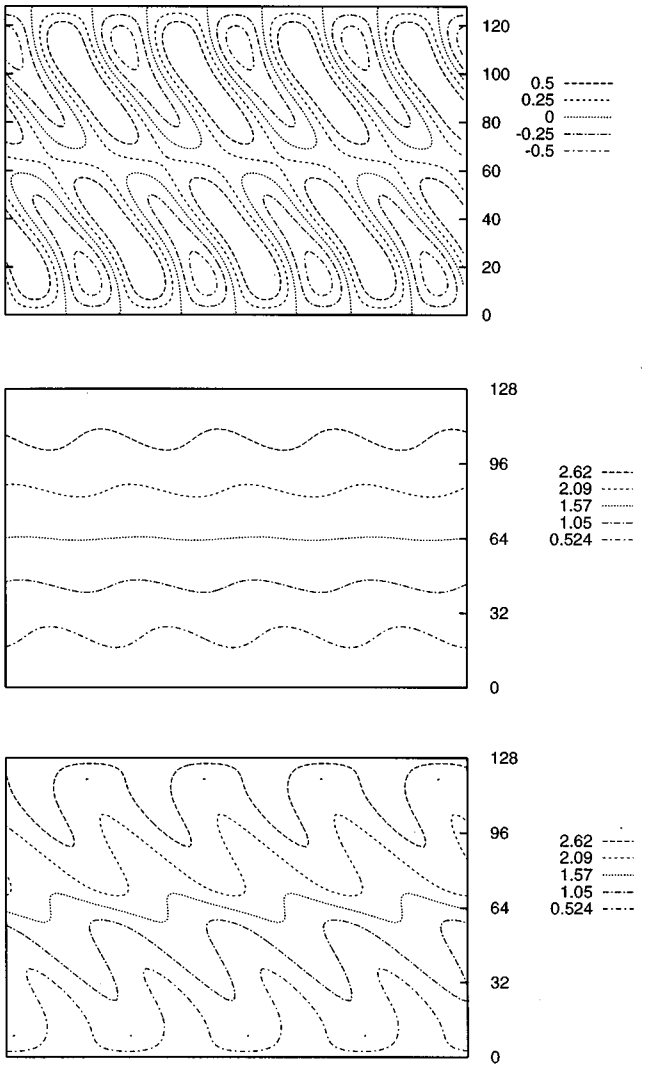

FIG. 5. Stream function, temperature, and salinity field (from top to bottom) at the time $t=13.1$. Same simulation as Fig. 1.

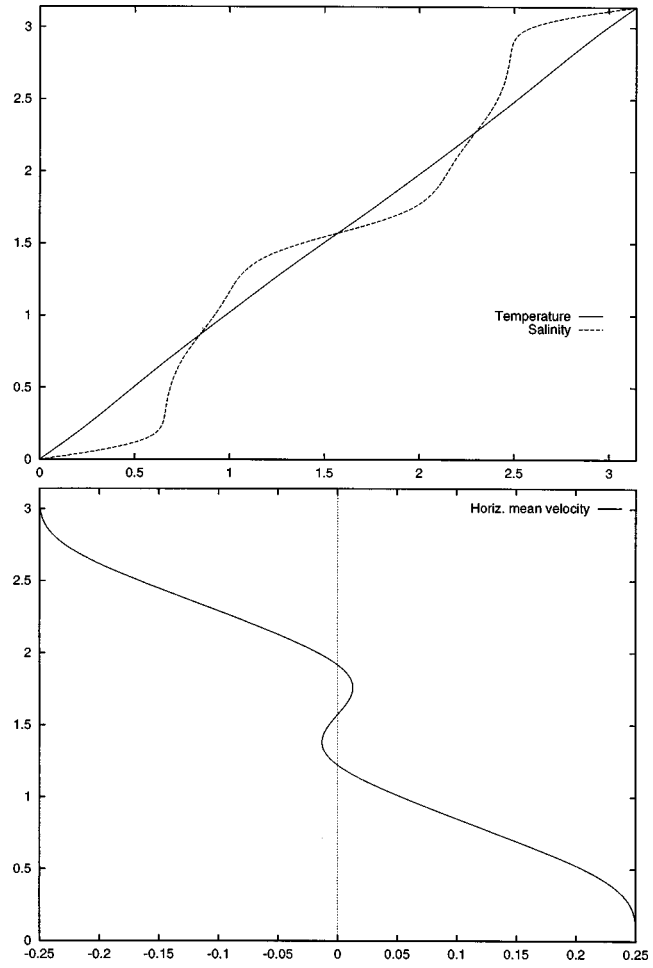

FIG. 6. Horizontally averaged profiles of temperature and salinity (top) and horizontal velocity (bottom) at the time $t=13.1$.

neous in the middle of the slab, and the flow field develops a double layer of convection cells (Fig. 5) which also appears in the salinity field.

Figure 6 showing $\overline{T}(z)$, $\overline{S}(z)$, and $U(z)$ reveals a different instability than the collective instability proposed by Stern.[4] It is not triggered by the horizontal shear between the ascending and descending fingers, but by the vertical shear imposed by the large scale horizontal velocity, U as in the nonoscillatory instability of Holyer.[6]

In a complete model one would expect to observe the onset of a salt-driven, larger-scale convection between the two layers of salt fingers, as observed in the experiments.[26] Here, with only one horizontal scale, a new set of fingers appears in the middle of the slab and grows up to the boundaries, replacing the old ones. As the fingers break, the large scale flow reaches its maximum strength but becomes severely damped right afterwards, when a new set of fingers forms.

The asymptotic behavior of the solutions of the nine-equation model does not seem to depend on the choice of the initial conditions; in particular it is independent of the shape of the initial average temperature and salinity profiles. However, with no added perturbation on the shear, the round-off errors alone did not trigger a large scale flow, at least on the time scales (up to 100 thermal times) that we explored.

We have performed some runs suppressing the large scale flow by omitting the first of Eqs. (7) and equating to zero the variable U in the others. With the same parameters as the simulation in Fig. 1, without the vertical shear, the fingers are stable. The numerical solutions that we observe are again a set of steady, straight convection cells. These can become unstable at much higher Rayleigh number because of an instability which appears to be generated by the horizontal shear between ascending and descending fingers. Figure 7 shows a snapshot of the fields for $R_T=50\,000$, $\mathcal{R}_\rho=1.5$, $\sigma=10$, $\tau=1/10$, and $\alpha=10$. Recirculation cells appear in the stream function and lead to the breaking of the salt fingers in a time-dependent way. Salinity is carried downward (and fresh water upward) in droplets that detach from the fingertips and slowly travel toward the boundaries.

The large scale flow need not be self-excited by the convective dynamics. In many situations of oceanographic interest it may be generated by other means. Hence, it is interesting to investigate the stability of the fingering convection under the presence of an externally imposed shear. We have introduced a linear large-scale flow using the transformation:

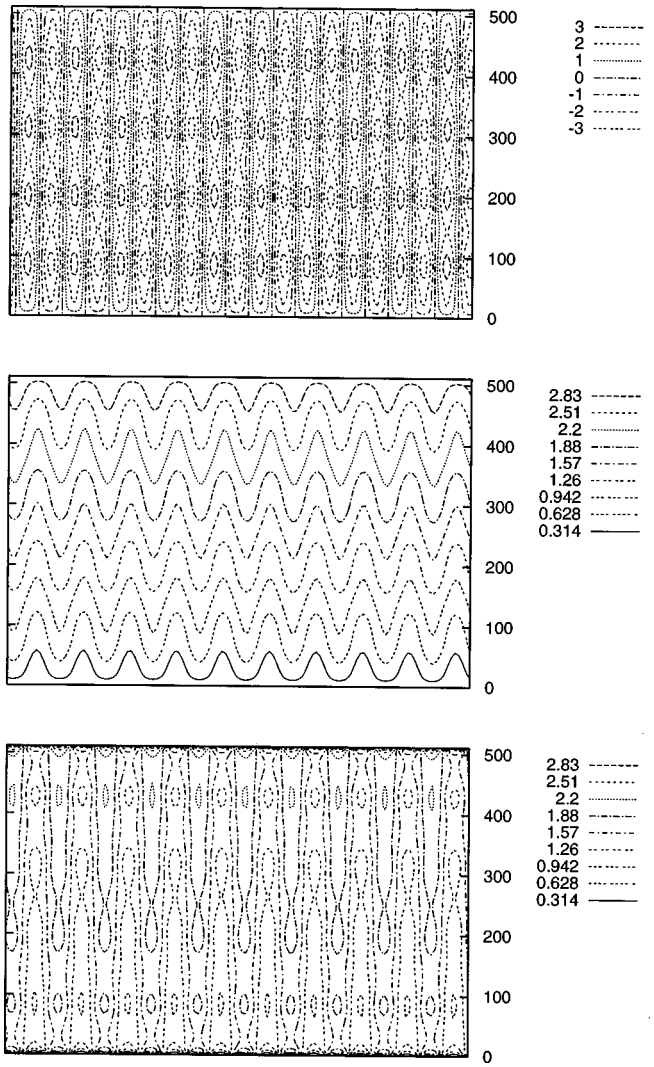

FIG. 7. Stream function, temperature, and salinity field (from top to bottom) for $R_T=50\,000$, $R_\rho=1.5$, $\sigma=10$, $\tau=1/10$, and $\alpha=10$ calculated with a simpler model that does not allow for a large-scale flow.

$$U(z,t)\rightarrow U(z,t)+U_0\left(\frac{2z}{\pi}-1\right). \tag{10}$$

To implement this in the code in a consistent way, the extra term has been expanded in a discrete cosine series, and then truncated to the maximum order allowed by the grid resolution.

With the same parameters as above and $\mathcal{R}_\rho=2$, a value of U_0 as small as 0.5 is enough to make the convection cells unstable. They break up in a way that is indistinguishable from that shown in Fig. 5, following a periodic cycle completely analogous to that described in the case of a self-excited shear. Higher density ratios require a stronger external shearing velocity to induce the sheared finger instability.

B. The vertical fluxes

To investigate the dependence of the convective fluxes of temperature and salinity on the Rayleigh number, a run has been performed in which the thermal Rayleigh number has been steadily raised from $R_T=500$ to $R_T=2500$ in 2000 thermal times while keeping the density ratio constant and

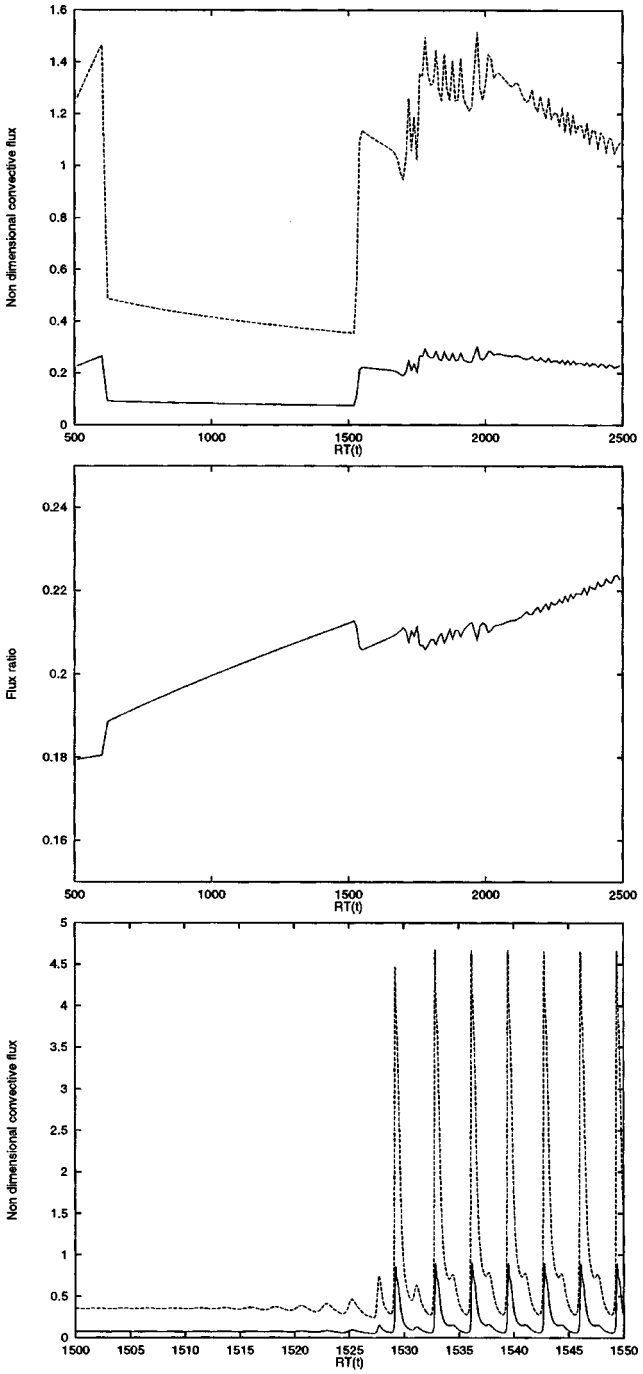

FIG. 8. The upper panel shows the nondimensional salinity (upper line) and the temperature (lower line) convective fluxes, as a function of the thermal Rayleigh number in a run where R_T increased at the rate of one unity every thermal time. The other parameters are $\mathcal{R}_\rho=2$, $\sigma=10$, $\tau=0.1$, and $\alpha=4$. The middle panel shows the flux ratio. The results are smoothed averaging the instantaneous fluxes over ten thermal times. The lower panel is a blow-up of the upper one that shows the onset of the fingering instability, and no smoothing is applied.

equal to 2. The fluxes have been measured by recording the values of $\partial_z\tilde{T}$ and $\partial_z\tilde{S}$ at the lower boundary. The results are shown in Fig. 8.

In the absence of a large-scale flow, the condition that the fluxes be independent of the domain height for asymptotically high Rayleigh numbers leads to fluxes varying as the 4/3 power of the imposed temperature and salinity

differences.[1] In our model equations, both the thermal and the salinity flux initially increase with R_T. However, this regime does not span a wide enough range of Rayleigh numbers to allow for a reliable estimate of the asymptotic value of the exponent. At the onset of the large-scale flow, the Nusselt number suddenly drops by about a factor 3 and slowly decreases as the Rayleigh number increases. This is seen in the model when the salinity effects are omitted as well and it is a result of the stability of shear flows at low Reynolds number combined with the two dimensionality of the model. This stabilizing effect of shear on convection has long been known.[27] The situation finally destabilizes at higher Rayleigh numbers and we see the development of a time dependence leading to an increase of the time-averaged fluxes with increasing Rayleigh number. The phenomenon consists of bursts of enhanced salinity and temperature transport signaling the growth of a new set of salt fingers, after a division of the fingering layer.

As R_T increases, the temporal dependence of the flow undergoes several changes, showing distinct periodic patterns separated by sharp transitions at critical values of the Rayleigh number, but no evidence of aperiodicity is found in the explored parameter range. The time-averaged fluxes generally decrease with R_T, but they abruptly increase when the temporal pattern changes. The flux ratio increases from about 0.18 at $R_T=500$ to about 0.22 at $R_T=2500$. These values are close to the theoretical values of 0.25 for maximum buoyancy flux fingers derived by Stern[28] and by Howard and Veronis[29] with different models.

At higher density ratios the fluxes are smaller, and the critical Rayleigh numbers for the onset of the large scale flow and for its time dependence are higher. The flux ratios, however, do not show big changes, decreasing by 5% as we pass from $\mathcal{R}_\rho=2$ to $\mathcal{R}_\rho=5$ at $R_T=1000$.

In the these simulations, although the Rayleigh number is increased very slowly, the onset of the large-scale flow is quite abrupt and it occurs at $R_T=600$. When the same kind of simulation is performed by lowering the Rayleigh number, the flow disappears at $R_T=220$, which is numerical evidence for a subcritical bifurcation to the shearing state.

IV. DISCUSSION

We have investigated the stability of salt fingers in a layer of finite vertical extent using model equations obtained from two-dimensional Boussinesq equations for doubly diffusive convection by a drastic truncation. Our representation of the flow consists of a single, finite, wavelength for the convective motion and it also includes a large-scale, horizontal velocity with vertical shear.

The solutions of this model show the growth of salt fingers from an initial two-layer setup. In a wide range of parameters the large scale flow is also excited in a way that is analogous to what happens in Rayleigh–Bénard convection. This leads to tilted fingers that recall the structures seen in the oceanic observations. At small density ratios ($\mathcal{R}_\rho=1.5$ in the simulations that we have shown) the vertical shear produced by the large-scale flow is able to break the set of salt fingers, temporarily homogenizing the temperature and the salinity in the middle of the slab. The same happens at higher density ratios when a strong enough external vertical shear is applied. This finding suggests that the structure of the staircase profiles of temperature and salinity observed in the oceans can be controlled by external factors besides the local convective parameters.

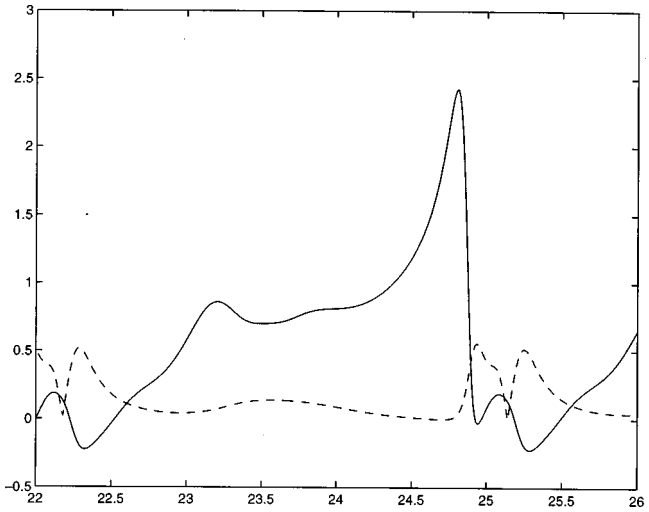

FIG. 9. Vertical gradient of horizontally averaged salinity (solid line) and Froude number (dashed line) vs time. One period is shown. For visualization purposes the Froude number has been multiplied by a factor 100.

However, a theory of finger instability based on a critical Froude number criterion seems to be inadequate because it neglects the feedback of the fingers on the vertical profiles of temperature and salinity in assuming that the destabilizing effect of the shear would consist only in a complete rollover of the fluid. As is shown in Fig. 9, there is no temporal coincidence between the layering events, signaled by the abrupt changes of $\partial_z S$ in the middle of the slab, and the maxima of the finger-shear Froude number,[12]

$$Fr=\frac{|\partial_z U \partial_x w|}{N_0^2}, \tag{11}$$

where the squared nondimensional buoyancy frequency $N_0^2=(-R_T+R_S)\sigma$ accounts for the average density gradient across the slab. The maxima of the Froude number are attained *after* the layering has occurred, when a new set of fingers grows, replacing the old one. Furthermore, the value of Fr never grows above a mere 5×10^{-3}.

Whether it is externally imposed or self-excited, the large-scale flow has the effect of engendering a recirculation of fluid in the fingertips of the cells with vorticity of the opposite sign as that of the shear. This is seen in Fig. 4, top panel. Layering occurs when the recirculation is able to build a salinity gradient in the middle of the slab strong enough to inhibit even the motion of the cells whose circulation is favored by the shear. This results in the two distinct sets of salt fingers, one above the other of Fig. 6. The enhanced salinity gradient also produces an unstable stratification, as in Fig. 10, which shows the vertical profile of the local, horizontally averaged, buoyancy frequency $N^2(z)=(-R_T\partial_z T+R_S\partial_z S)\sigma$. Inside the unstably stratified layer the conditions are favorable to the onset of a larger scale, Bénard-like con-

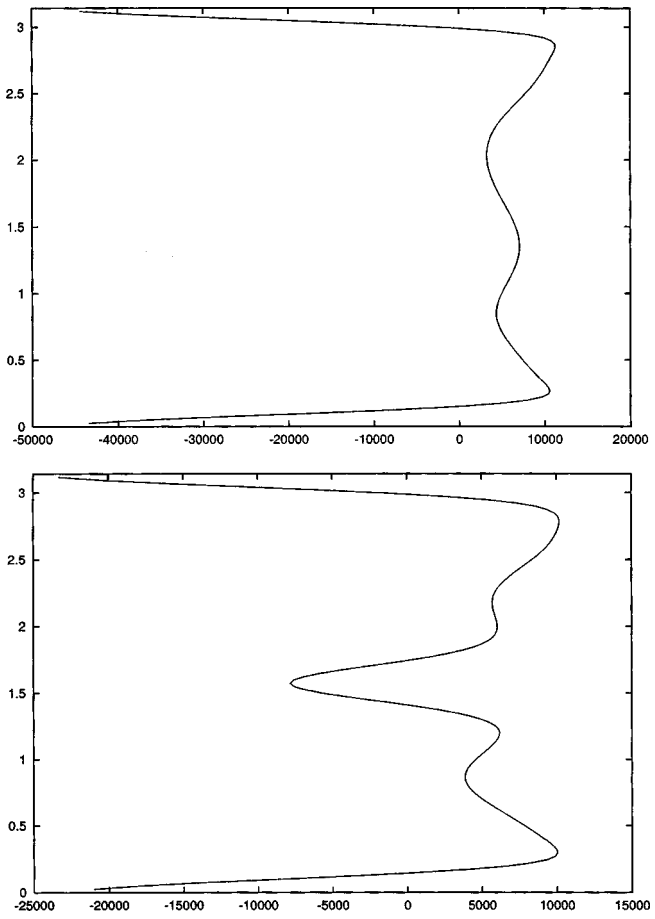

FIG. 10. Squared buoyancy frequency N^2 (horizontal axis) vs height (vertical axis) at the times $t=1$ (top panel) and 1.31 (bottom panel).

vection, as is observed in the laboratory experiments. Our model does not have a mode that could represent this kind of convection, and new fingers grow across the slab, replacing the old ones.

Strong changes in the vertical fluxes of salinity and temperature are observed at the onset of the large-scale flow. No scaling law is found in our simulations for the fluxes as a function of the Rayleigh number. Although the precise behavior of this relationship is very likely model dependent, it suggests that the popular 4/3 law is destroyed by a vertical shear, as is observed in Rayleigh–Bénard convection.

The shear-induced breakup occurs well before the onset of a collective instability of the kind studied by Stern and Holyer that may be recovered by a simpler model that makes no allowance for the large-scale flow. Whether this conclusion remains true for the full Boussinesq equations remains to be seen. Further studies are also needed to investigate how much a third dimension would affect the scenario that we have sketched. Here we simply note that if an externally imposed shear favors the formation of rolls, as in Linden's experiments, our two dimensional approach would have a direct applicability.

ACKNOWLEDGMENTS

This work was begun during the 1996 Geophysical Fluid Dynamics program at the Woods Hole Oceanographic Institution. We are especially grateful to Mike Shelley who taught us much about the art of writing spectral codes. We also thank Louis Howard, Barry Ruddick and George Veronis for helpful discussions.

[1] J. S. Turner, *Buoyancy Effects in Fluids* (Cambridge University Press, Cambridge, 1979).
[2] E. A. Spiegel, ''Convection in stars II. Special effects,'' Annu. Rev. Astron. Astrophys. **10**, 261 (1972).
[3] R. W. Schmitt, ''Double diffusion in oceanography,'' Annu. Rev. Fluid Mech. **26**, 255 (1994).
[4] M. E. Stern, ''Collective instability of salt fingers,'' J. Fluid Mech. **35**, 209 (1969).
[5] J. Y. Holyer, ''On the collective instability of salt fingers,'' J. Fluid Mech. **110**, 195 (1981).
[6] J. Y. Holyer, ''The stability of long, steady, two-dimensional salt fingers,'' J. Fluid Mech. **147**, 169 (1984).
[7] E. Kunze, ''Limits on growing, finite length salt fingers: a Richardson number constraint;'' J. Mar. Res. **45**, 533 (1987).
[8] R. B. Lambert and J. W. Demenkow, ''On the vertical transport due to fingers in double diffusive convection,'' J. Fluid Mech. **54**, 627 (1971).
[9] R. W. Griffiths and B. R. Ruddick, ''Accurate fluxes across a salt–sugar finger interface deduced from direct density measurements,'' J. Fluid Mech. **99**, 85 (1980).
[10] R. Krishnamurti and L. N. Howard, ''Large scale flow in turbulent convection,'' Proc. Natl. Acad. Sci. USA **78**, 1981 (1981).
[11] P. F. Linden, ''Salt fingers in a steady shear flow,'' J. Geophys. Res. **6**, 1 (1974).
[12] E. Kunze, ''A proposed flux constraint for salt fingers in shear,'' J. Mar. Res. **52**, 999 (1994).
[13] L. N. Howard and R. Krishnamurti, ''Large scale flow in turbulent convection: a mathematical model,'' J. Fluid Mech. **170**, 385 (1986).
[14] K. B. Hermiz, P. N. Guzdar, and J. M. Finn, ''Improved low-order model for shear flow driven by Rayleigh–Bénard convection,'' Phys. Rev. E **51**, 325 (1995).
[15] J.-L. Thiffeault and W. Horton, ''Energy-conserving truncations for convection with shear flow,'' Phys. Fluids **8**, 1715 (1996).
[16] E. N. Lorenz, ''Deterministic nonperiodic flow,'' J. Atmos. Sci. **20**, 130 (1963).
[17] J.-P. Zahn, J. Toomre, E. A. Spiegel, and D. O. Gough, ''Nonlinear cellular motions in Poiseuille channel flows,'' J. Fluid Mech. **64**, 319 (1974).
[18] D. O. Gough, E. A. Spiegel, and J. Toomre, ''Modal equations for cellular convection,'' J. Fluid Mech. **68**, 695 (1975).
[19] J. Toomre, D. O. Gough, and E. A. Spiegel, ''Time-dependent solutions of multimode convection equations,'' J. Fluid Mech. **125**, 99 (1982).
[20] D. O. Gough and J. Toomre, ''Single-mode theory of diffusive layers in thermohaline convection,'' J. Fluid Mech. **125**, 75 (1982).
[21] B. Castaing, G. Gunaratne, F. Heslot, L. Kadanoff, A. Libchaber, S. Thomae, X.-Z. Wu, S. Zaleski, and G. Zanetti, ''Scaling of hard thermal turbulence in Rayleigh–Bènard convection,'' J. Fluid Mech. **204**, 1 (1989).
[22] J. M. Massaguer, E. A. Spiegel, and J.-P. Zahn, ''Convection-induced shears for general planforms,'' Phys. Fluids A **4**, 1335 (1992).
[23] J. Werne, ''Plume model for the boundary-layer dynamics in hard turbulence,'' Phys. Rev. E **49**, 4072 (1994).
[24] C. Canuto, M. Y. Hussaini, A. Quarteroni, and T. A. Zang, *Spectral Methods in Fluid Dynamics* (Springer, Berlin, 1988).
[25] Double-diffusive processes 1996 summer study program in geophysical fluid dynamics, edited by S. Meacham and D. Tucholke, Woods Hole Oceanography Institute Technology Report WHOI-97-10, 1997 (unpublished).
[26] P. F. Linden, ''The formation of the banded salt finger structure,'' J. Geophys. Res. **83C**, 2902 (1978).
[27] D. Avsec, ''Tourbillons Thermoconvectifs dans l'Air,'' Facultè des Sciences de l'Universitè de Paris (1939).
[28] M. E. Stern, ''Maximum buoyancy flux across a finger interface,'' J. Mar. Res. **34**, 95 (1976).
[29] L. N. Howard and G. Veronis, ''The salt-finger zone,'' J. Fluid Mech. **183**, 1 (1987).